Self-assembly of gold nanoparticles into nanoholes through annealing in the fabrication of square lattices of nanocylinders

Xinping Zhang (张新平)[1], Baoquan Sun[2], Hongcang Guo[3], Jinrong Tian (田金荣)[1], Yanrong Song (宋晏蓉)[1], and Li Wang (王 丽)[1]

[1]*College of Applied Sciences, Beijing University of Technology, Beijing 100022*

[2]*Cavendish Laboratory, University of Cambridge, Cambridge CB3 0HE, UK*

[3]*Fourth Physics Institute, University of Stuttgart, Stuttgart D-70569, Germany*

Received July 9, 2007

We demonstrate the self-assembly of solution-processible gold nanoparticles into the nanoholes consisting of patterned substrate through annealing, which facilitates successful fabrication of square lattices of gold nanocylinders with a period of 350 nm, a height of about 200 nm, and an aspect ratio larger than 2.

OCIS codes: 240.6680, 220.4610, 220.0220.

Metallic photonic crystals[1,2] based on the particle plasmon resonance of metallic nanocylinders have potential applications in selective spectral absorption, all-optical switching[3], biosensors, and distributed feed-back lasers. The conventional method to produce metallic photonic crystals is using electron-beam (e-beam) lithography followed by gold evaporation and lift-off[1,2]. However, the expensive e-beam writer and vacuum evaporator involved in this technique, as well as the complicated vacuum evaporation procedures and time-consuming writing process, limit the application, especially in the fabrication of large-area (diameter $>$ 5 mm) structures. Dry etching techniques[4] also require expensive evaporation and etching equipment. In contrast, a solution-processible method in combination with interference lithography is a very simple, low-cost, and high-speed approach[5], which involves only simple chemical synthesis, spin-coating, and subsequent low-temperature ($\leq$ 260 °C) annealing processes, thus enables mass fabrication of photonic crystal devices. It has been proposed that the confinement mechanism is based on the periodic modulation of the surface energy by the mask grating in addition to a natural process provided by the grating grooves, which induces dewetting off the top surface of the grating.

In this work we demonstrate that a further mechanism plays a dominant role in the fabrication of the two-dimensional (2D) metallic photonic structures, which is the large surface tension introduced by the molten gold through annealing. Thus, 2D square lattices of gold nanocylinders have been fabricated with an aspect ratio larger than 2.

The first stage of the fabrication is the preparation of a mask grating using interference lithography in photoresist (PR), which consists of nanoholes with a period of 350 nm, a modulation depth of about 200 nm, and an area as large as 20 mm^2. The mask grating is fabricated on a layer of indium tin oxide (ITO) with a thickness of 200 nm deposited on a 1-mm-thick glass substrate. Further details about the fabrication of this kind of PR grating are described in Ref. [4]. In the second stage, gold colloid with a concentration of 50 mg/mL is spin-coated onto the top surface of the mask grating at a speed of 2000 rpm for 30 s before an annealing process at 260 °C. The preparation of the gold nanoparticle colloid is described in detail in Ref. [5]. After the annealing process, almost all of the gold has been confined into the nanoholes, forming periodically distributed gold nanocylinders. Thus, we succeeded in producing large-area well-defined 2D metallic photonic crystal structures that show very well defined particle plasmon resonance spectrum. The microscopic and optical properties of the resultant photonic crystal device show convincingly that our solution-processible method is comparable to any other techniques, including those based on e-beam lithography[1,2], dry etching[4], electrodeposition[6,7], and electric-field-assisted dissolution[8], in producing high-quality metallic photonic crystals, while it has the apparent advantages of simplicity, low cost, and high speed.

We have demonstrated that ITO has much higher surface energy than PR so that the gold colloid solution tends to dewet off the PR surface and aggregate onto the ITO surface[5]. To confirm this in the 2D fabrication, we used relatively low concentration of the gold colloid (50 mg/mL) and large holes (400 nm in diameter) that form the mask grating. Figure 1 shows the corresponding

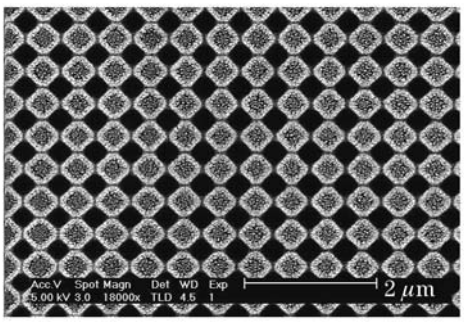

Fig. 1. SEM image of the gold nanostructures fabricated on 2D mask gratings of nanoholes with a diameter as large as 400 nm and a depth of 100 nm.

1671-7694/2007/110657-03 © 2007 Chinese Optics Letters

scanning electron microscopy (SEM) image of 2D structures with a period of about 500 nm and annealed at 260 °C for about 5 minutes. The modulation depth of the nanoholes was about 100 nm. The dark area in Fig. 1 is covered with PR, while the gold has filled the ITO-bottomed hole structures, and the annealed gold is displayed as bright spots in Fig. 1. Clearly, the gold has been confined completely into the holes, confirming convincingly the confinement mechanism based on the surface-energy difference between the ITO and the PR for such a configuration. Because of the relatively large period and the large duty cycle (ITO/whole structure area $> 70\%$) of the mask grating, as well as the low concentration of the gold colloid, the gold nanostructure was not continuous, as shown in Fig. 1. In order to investigate the plasmon resonance properties of the metallic nanostructures in the visible spectral range, all gold in the nanoholes is required to be melted into a solid entity with a diameter generally smaller than 200 nm. Moreover, as mentioned above, it is more interesting to produce 2D lattices with high aspect ratio. Taking these considerations into account, we need to largely reduce the diameter and increase the modulation depth of the nanoholes. As a result, during the spin-coating process the gold colloid will "feel" significantly reduced confinement strength induced by the surface-energy difference between the PR and the ITO. However, our experiments revealed that an even stronger confinement mechanism based on the large surface energy of the melted gold during the annealing process enabled successful fabrication of 2D plasmonic metallic photonic crystals.

Figure 2 shows the SEM image of the 2D photonic crystal structures, which demonstrates nearly complete confinement of the gold into the nanoholes of the mask grating, although the nanoholes were measured to take up less than 12% of the whole structure area. The gold nanocylinders have a mean diameter of about 100 nm. Homogeneous distribution of these gold nanocylinders confirms the success of this fabrication method. Atomic force microscopy (AFM) measurement showed that the top surface of the gold is less than 20 nm above the mask grating. To understand this, we have to consider the annealing-induced further aggregation of the gold after filling out the nanoholes during the spin-coating process. Because of the much higher surface energy of the ITO than the PR[5], as well as a natural confinement mechanism provided by the nanoholes, a large portion of the gold nanoparticles has been confined into the nanoholes during spin coating. However, the small nanoholes could not hold all of the gold nanoparticles, especially at a high concentration of the colloid. Furthermore, with accumulation of the gold nanoparticles into the nanoholes, the surface energy difference between the ITO and the PR becomes weaker and weaker as sensed by the gold colloid. Nevertheless, the extra amount of the gold nanoparticles tends to populate around the nanoholes due to the aggregation-induced mass flow of the colloid in the spin-coating stage. Consequently, when the sample was heated and all of the gold nanoparticles became melted in the annealing process, large droplets of melted gold formed in the nanoholes tended to draw the surrounding smaller ones due to the large surface energy of the melted gold and the close contact between the nanoparticles, forming even larger droplets. In the cooling process, the final large droplets were solidified to form gold cylinders, which might have larger volumes than the nanoholes and thus can stick out of the mask grating surface.

Figure 3 shows the optical extinction spectrum of the spin-coated gold nanoparticle film before and after the annealing process. The well-defined particle plasmon resonance spectrum of the gold nanocylinders is peaked at about 740 nm and has a bandwidth at full-width at half-maximum (FWHM) of about 140 nm, indicating high quality of the photonic crystal structure of gold nanocylinders.

Further experiments (not shown here) have confirmed that the natural confinement mechanism by the periodic mask structure during the spin coating process and the further aggregation of the melted gold nanoparticles during the annealing stage have played crucial roles in the fabrication of the 2D device, where we used a mask grating without being developed down to the ITO surface so that the higher surface energy of the ITO could not be felt by the colloidal solution. Whereas, we could still observe well-defined gold nanocylinders embedded into the mask gratings and measure strong optical response of the particle plasmon resonance.

Although the dimension of the gold nanocylinders can also be tuned by controlling the duty cycle of the mask grating, changing the concentration of the gold colloid solution is a more flexible and more reproducible method for tuning the spectral properties of the particle plasmon resonance. The microscopic measurement in Fig. 4(a) and optical properties in Fig. 4(b) indicate that very low

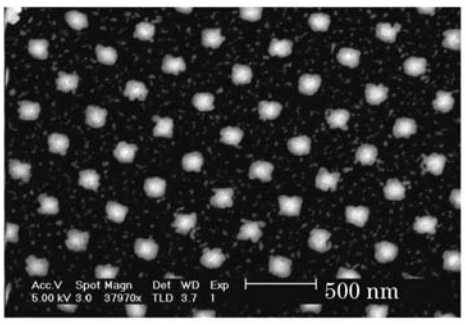

Fig. 2. SEM image of the square lattices of gold nanocylinders fabricated using a gold colloid concentration of 50 mg/mL.

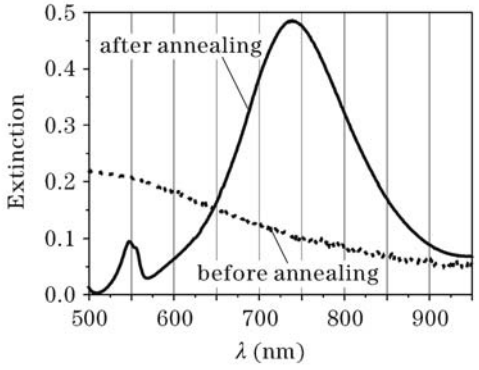

Fig. 3. Optical extinction spectrum measurements of the square lattices shown in Fig. 2 before (dashed curve) and after (solid curve) the annealing process.

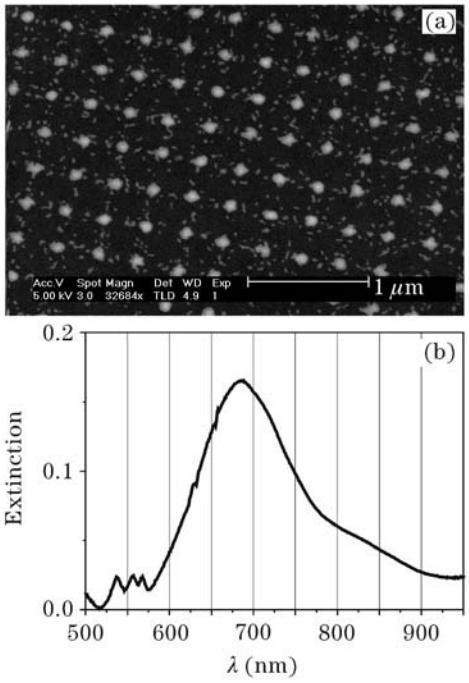

Fig. 4. (a) SEM image of the square lattices of gold nanocylinders fabricated using a low gold colloid concentration of 26 mg/mL; (b) optical extinction measurement of the structures in (a).

concentration (< 26 mg/mL) can produce satisfying 2D structures, implying even lower cost of this technique. This is based on the much lower duty cycle of the 2D than the 1D structures. With reducing the diameter of the nanoholes in the mask grating and the concentration of the gold colloid, the particle plasmon resonance shown in Fig. 4(b) shifts to the blue side with respect to the results shown in Fig. 3.

In conclusion, we have demonstrated the fabrication of 2D waveguided metallic photonic crystals using solution-processible gold nanoparticles. The optical extinction spectrum measurements showed well-defined particle plasmon resonance of the individual gold nanocylinders, indicating high-quality fabrication of the 2D structures. The strong aggregation of the gold nanoparticles during the annealing process, which is based on the large surface energy of the molten gold, has been the dominant confinement mechanism in the 2D fabrication. Changing the concentration of the gold nanoparticle colloid enabled flexible tuning of the particle plasmon resonance.

The authors thank Professor Harald Giessen and Professor Richard Friend for very helpful discussions. This work was supported by the National Natural Science Foundation of China under Grant No. 10744001. X. Zhang's e-mail address is zhangxinping@bjut.edu.cn.

References

1. A. Christ, S. G. Tikhodeev, N. A. Gippius, J. Kuhl, and H. Giessen, Phys. Rev. Lett. **91,** 183901 (2003).
2. A. Christ, T. Zentgraf, J. Kuhl, S. G. Tikhodeev, N. A. Gippius, and H. Giessen, Phys. Rev. B **70,** 125113 (2004).
3. D. Nau, R. P. Bertram, K. Buse, T. Zentgraf, J. Kuhl, S. G. Tikhodeev, N. A. Gippius, and H. Giessen, Appl. Phys. B **82,** 543 (2006).
4. H. C. Guo, D. Nau, A. Radke, X. P. Zhang, J. Stodolka, X. L. Yang, S. G. Tikhodeev, N. A. Gippius, and H. Giessen, Appl. Phys. B **81,** 271 (2005).
5. X. Zhang, B. Sun, R. H. Friend, H. Guo, D. Nau, and H. Giessen, Nano Lett. **6,** 651 (2006).
6. N. S. Pesika, A. Radisic, K. J. Stebe, and P. C. Searson, Nano Lett. **6,** 1023 (2006).
7. I. B. Diliansky, A. Shishido, I.-C. Khoo, T. S. Mayer, D. Pena, S. Nishimura, C. D. Keating, and T. E. Mallouk, Appl. Phys. Lett. **79,** 3392 (2001).
8. A. Abdolvand, A. Podlipensky, S. Matthias, F. Syrowatka, U. Gösels, G. Seifert, and H. Graener, Adv. Mater. **15,** 2983 (2005).